DOI: 10.1002/anie.201207693

Printed Electronics

From Paper to Structured Carbon Electrodes by Inkjet Printing**

*Stefan Glatzel, Zoë Schnepp, and Cristina Giordano**

Electronics undoubtedly provide the foundation of information technology, uniting efforts from a wide range of scientific disciplines.[1] Generations of materials scientists have strived to develop new processes to meet the demand for more advanced materials while providing enhanced processability and making microelectronics even more affordable. However, microelectronics processing is highly integrated, and the process chain is not readily accessible. Furthermore, there is a trend towards simpler approaches, both to reduce the price and environmental impact and to allow more flexible layout and smaller numbers of units (down to single, custom-designed units), thus accelerating development processes and leading to new applications. Functional printing techniques have been identified as the most promising approach for this type of electronics.[2] To date, processes are often difficult to scale up and, most importantly, they almost exclusively use thermally unstable precursors (usually the support). This has hampered the integration of printing techniques with well-established high-temperature processing techniques, a key requirement for future electronics. Herein we describe a solution to these problems, without sacrificing simplicity, by using a paper support and catalytic ink as two "reactants" to generate functional carbon/ceramic arrays and three-dimensional structures. This simple "beyond the lab" process with off-the-shelf equipment is suitable for the large-scale and high-temperature production of materials with applicationas as electrodes and catalysts.

The printing of chemically active substances has spurred key advances in several fields including colloid science and biopharmacy,[3] in the construction of microstructured functional materials by means of sol–gel chemistry,[4] in the manufacture of functional coatings,[5] and in ionogel-based flexible electronics.[6] This approach has already been used to generate a wide variety of materials and properties.[7] Although some work has been done in the field of carbon conductors,[8] it relied on the dispersal and printing of preformed carbon structures rather than an in situ process. Furthermore none of these methods addressed the application to the existing industry-standard high-temperature processing used in microelectronics manufacture.

In a first step, we filled the cartridges of a commercial inkjet printer (see Figure S1 in the Supporting Information) with a metal catalyst precursor and printed defined two-dimensional, lateral patterns on clean cellulose paper. The resolution here is controlled by the printing process and above all by the paper structure. In a possible second step, this paper can be shaped, processed, or simply folded to a desired three-dimensional structure. Final thermal conversion of this structure then leads to the reaction of the catalytic ink with the paper, thus creating in this case conductive structures of iron carbide in graphitic carbon.

The precision with which the spatial conformation of a 3D paper object can be retained was shown by folding a paper crane (see Figure 1). We used a sheet of filter paper, folded it into an origami crane, soaked it with the catalytic ink (see below), and then calcined it under inert atmosphere. Finally, the calcined crane was coated with copper to demonstrate the homogeneity of the final structure and the high degree of processability that is possible with this system. Similarly, the catalytic carbonization of thin tissue paper demonstrates the flexibility and durability of the final material for improved handling and broader applications (see Figure 1E and Figure S4 in the Supporting Information). All experiments were repeated in parallel with powdered microcrystalline cellulose instead of filter paper (using the same ink but simply soaking the cellulose powder) in order to establish whether this process can be scaled up to larger quantities and whether the actual fiber form of the cellulose is required, for example, as a structural template. This scaling was possible, and the cellulose powder proved to be a good model system.

A catalytic ink of iron(III) nitrate (14 g) in water (15 mL) was transferred into an empty ink cartridge with a syringe. The cartridge was placed back into the printer and could be used directly. For the sake of simplicity and to exclude the possibility that additives in printer paper influence the product formation, we mounted a piece of pure, cellulose filter paper (laboratory grade) on a sheet of standard A4 printer paper (see Figure S2 in the Supporting Information). The printed area (Figure 2A) was cut out and placed between two slides of quartz glass to prevent wrinkling during subsequent carbonization. Conversion to Fe_3C, graphitic carbon, and amorphous carbon was achieved by a single heating step at 10 K min^{-1} to 800 °C under N_2 flow followed immediately by cooling to room temperature (Figure 2B). The experiments were also performed with a heating rate of 2 K min^{-1} with no difference in the produced products.

The final product shrinks to approximately 60% of the initial dimensions on the centimeter or micrometer scale (see Figure S3 in the Supporting Information). The microscopic

[*] S. Glatzel, Dr. C. Giordano
Colloid Chemistry, Max Planck Institute of Colloids and Interfaces
Am Mühlenberg 1, 14476 Golm (Germany)
E-mail: cristina.giordano@mpikg.mpg.de
Dr. Z. Schnepp
International Center for Young Scientists
National Institute for Materials Science
1-2-1 Sengen, Tsukuba, Ibaraki, 305-0047 (Japan)

[**] We thank Prof. Markus Antonietti for fruitful discussions and kind help, and Rona Pitschke, Heike Runge, and. Katharina Otte for SEM and TEM measurements. This work was supported financially by the Max Planck Society (C.G. and S.G.) and National Institute for Materials Science, International Center for Young Scientists (Z.S.).
Supporting information for this article is available on the WWW under http://dx.doi.org/10.1002/anie.201207693.

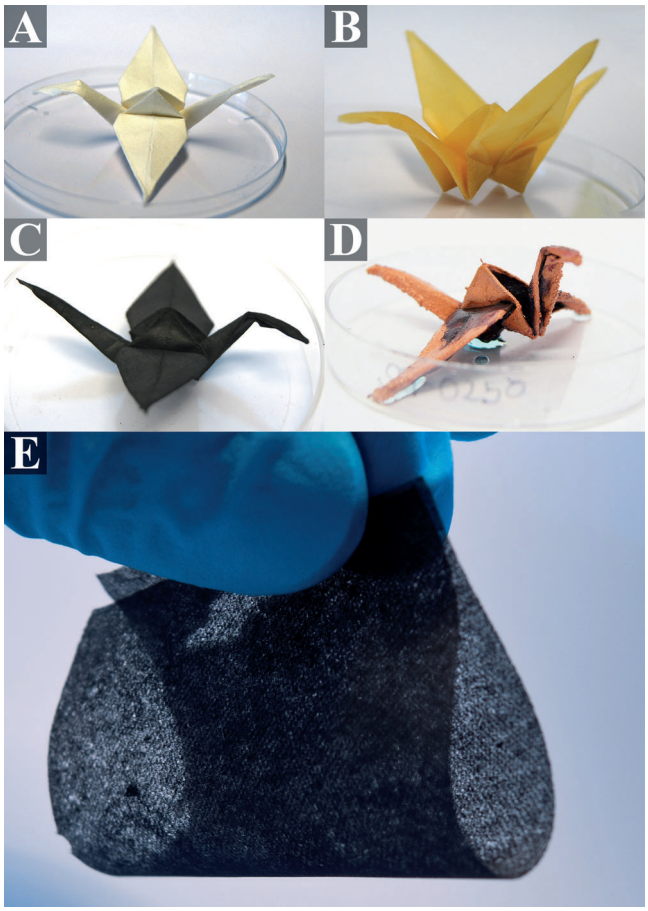

Figure 1. Illustration of the processability. A folded piece of filter paper and a flexible single-layer tissue were used to demonstrate the shape retention. Folded origami crane (A), after soaking with the iron precursor solution (B), after calcination under N_2 flow (C), and after copper deposition (D). E) Example of a fully flexible sample derived from ultrathin paper.

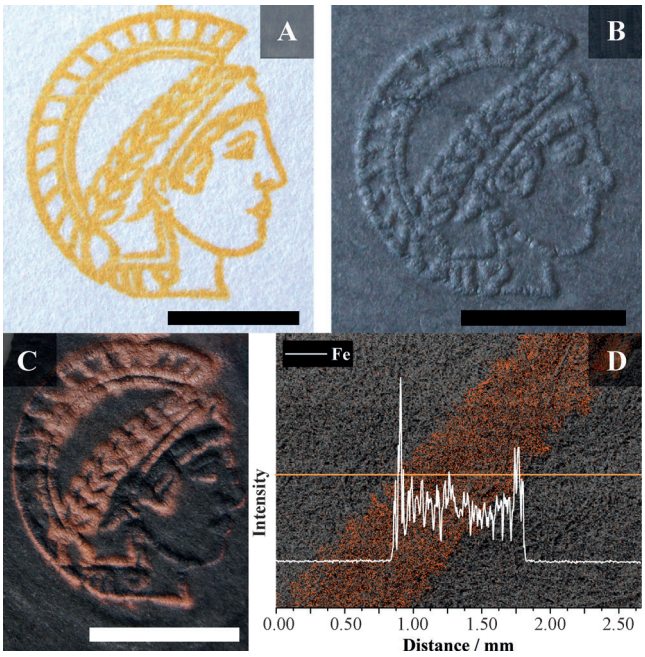

Figure 2. Preparation of the patterned electrodes. Printed sample (A), after calcination (B), after copper deposition (C); the scale bar in each picture represents 1 cm. D) Line EDX for iron (white plot) along the orange line and elemental mapping of the same area (carbon in gray, iron in red) both conducted on a sample line that was printed and calcined.

texture and macroscopic shape are retained entirely. After calcination, the printed and nonprinted areas are noticeably different: the nonprinted areas shrink slightly more, thus giving the overall structure an "embossed", three-dimensional appearance. In addition, the printed areas are apparently composed of a rather stable, hard carbon hybrid whereas the nonprinted areas are made up of amorphous carbon; neither space-resolved X-ray diffraction (XRD) (Figure 3A) nor Raman spectroscopy showed clear signs of local carbon order (Figure S5). However, the areas treated with the catalytic ink underwent substantial changes in morphology. When one observes the structure on the nanometer scale it becomes apparent that the cellulose, under influence of the catalytic ink, does not turn into amorphous carbon, but rather exclusively into rolled or closed graphene nanostructures (see Figure 3B). The overall composite consists of two types of components: iron carbide particles encased by a high-purity multilayer graphitic carbon shell. The other structural element is rolled and crumpled graphene sheets. Although the sheets are rolled up, in some cases 90° bends in the carbon layers have been observed which supports the presence of graphitic layers rather than purely tubular structures.

The printed regions of the paper exhibited 30-times higher electrical conductivity than the amorphous, nonprinted parts (18 $S\,cm^{-1}$ versus 0.6 $S\,cm^{-1}$), enabling selective coating of the printed parts. Therefore, to demonstrate the integrity and spatial isolation of this conductive network within the amorphous carbon matrix, we performed the electro-deposition of copper, which results in even, fine copper lines (Figure 2C).

To explore the mechanism of the iron-catalyzed transformation of cellulose, we conducted a thorough investigation of the system by using thermogravimetric analysis (TGA), XRD experiments (with samples cooled down from various temperatures in order to obtain a full temperature-dependent profile of the reaction), transmission electron microscopy (TEM) on microtomed quenched samples (Figure S6), and in situ TEM at the reaction temperature (Figure 4 and Figure S7 and a video in the Supporting Information).

Thermogravimetric analysis showed that the initial decomposition of the cellulose occurs between 250 °C and 400 °C, with the main mass loss due to dehydration at 337 °C. A second pronounced step at 610 °C (Figure S8) was identified as the carbothermal reduction of iron oxide to elemental iron and carbon oxides. This is supported by XRD patterns of samples quenched at 100 °C intervals (Figure S9), which show the crystallization of iron oxide at approximately 500 °C and the subsequent formation of iron carbide upon further heating along with the appearance of a pronounced peak attributed to graphitic carbon at about 26°. The XRD patterns

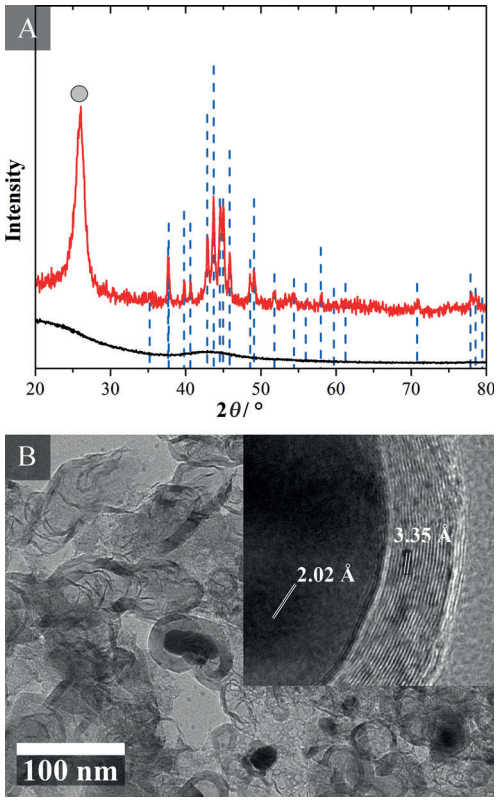

Figure 3. A) XRD patterns of the graphitized areas (red) with a reference pattern for Fe_3C (blue, ICDD 00-34-0001) and of the nongraphitized areas (black); the peak markedwith a gray circle at $2\Theta = 26°$ is attributed to graphitic carbon (ICDD 04-15-2407). B) Ultramicrotome TEM of a graphitized area and a high-resolution micrograph with labeled lattice fringes (inset).

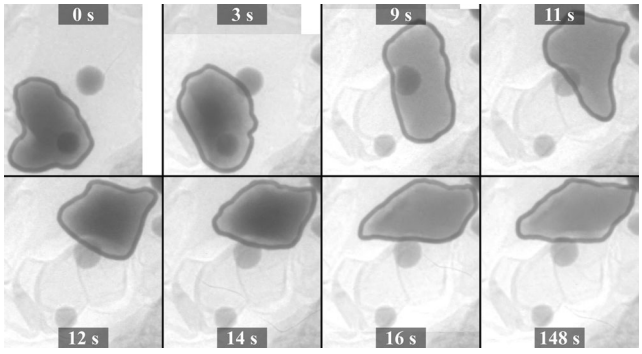

Figure 4. Frames taken from an in situ TEM video (complete video is provided in the Supporting Information) depicting the initially fast movement of the 50–200 nm iron–carbon droplets which comes to an abrupt halt when the particle is surrounded by already graphitized areas.

show peak broadening with increasing temperature for the iron oxide phase, indicating an initially surprising shrinkage of the iron oxide crystallites between 600 and 700 °C. At temperatures above 800 °C, the gradual decomposition of iron carbide into graphitic carbon and elemental iron is observed as expected.[9]

The TEM micrographs on quenched samples reveal that in a first step iron-containing nanoparticles are formed on the surface of the carbonized cellulose fibers, which then in a fast process (10 min at maximum) "eat up" (convert) the fibers, leaving behind the well-ordered crumpled and rolled graphite structures (Figure 3B and Figure S6 in the Supporting Information).

Based on these observations it is clear that iron nitrate is converted to iron oxide nanoparticles, which are then carbothermally reduced to metallic iron-containing nanoparticles, the exact composition and state of which is still subject of intense debate.[10] These then can dissolve the amorphous carbon from cellulose and recrystallize it in the form of ordered graphene nanostructures with higher mechanical stability and electrical conductivity. This dissolution/precipitation mechanism in the Fe/C system is known from the formation of carbon nanotubes,[11] and was also observed for the formation of extended graphene stacks from polymer ionic liquids.[12] The current system provides exciting additional details of this process.

We propose that the reaction proceeds via a liquid eutectic metal "droplet" (approximately 50:50 mixture of iron and carbon[9–11]), which is also evident, from a structural point of view, in some final Fe_3C nanostructures after quenching (Figure S10). When the samples cools, more graphitic carbon is formed through delamination of thin surface layers from the carbide and subsequent formation of crystalline Fe_3C nanoparticles (Figure 3B, inset) in the resulting hollow carbon shells. These arise from the decomposition of the eutectic into two crystalline subphases, with around 50 mol% carbon (as judged by the relative volume contribution of those two phases). Interestingly the crystalline Fe_3C particles are smaller than the former liquid eutectic particles, leaving behind the appropriate cavity.

The most impressive proof for this mechanism is given by in situ TEM between 700 and 800 °C, which allows the direct observation of the formation of the final product (Figure 4 and Figure S7 and video in the Supporting Information). The liquid eutectic "droplets" roughly 50–200 nm in size can be followed as they "eat up" the amorphous carbon, leaving behind a trail of crystallized graphitic carbon; the driving force is the lower free energy of the perfect graphitic structures. Note that the melting point of pure iron is 1538 °C, with technical iron alloys melting at temperatures down to 1270 °C. Surface effects as well as the stabilization of this very unusual eutectic carbon/iron phase by nanoeffects thereby lower the melting point by at least 500 °C, which is unexpected.

Because of the apparently high mobility of the liquid iron "nanodroplets", we felt it was necessary to assess the quality of the border of graphitization between the areas printed with the catalytic ink and the nonprinted areas. The results showed that the eutectic particles travel at most a few hundred nanometers into the amorphous region (see Figures S11–S13).

In conclusion, we have presented a remarkably simple and general procedure to turn ordinary cellulose into mesostructured graphene nanoassemblies that retain structural properties with very high accuracy. As the iron catalyst can be

printed on the paper, these materials are also available in 2D-patterned arrays, for example, for microstructured electrodes through facile ink-jet processing techniques. The leftovers of the catalyst are retained in the final material as carbon-encapsulated iron carbide nanohybrids which makes them noncritical for most of the further processes and applications.

The use of such textured objects was exemplified by the targeted electro-deposition of copper, turning the conductive carbon pattern into metallic objects. However, more refined applications such as structured catalytic arrays and paper-based electronics can be envisaged. It must also be stated that the procedure is not only remarkably cheap, but also fast: even under simple laboratory conditions, the graphic design, printing, calcination, and electro-deposition of a de novo array or electrode takes less than 2 h, in a potentially highly parallel fashion. Such "converted paper" structures have tremendous potential as electrodes for fuel cells and batteries, where the co-printing of the appropriate metals and metal salts (e.g. Pt or Li) can directly lead to micrometer- (paper) to millimeter-thick (cardboard) functional devices, made in a most simple fashion.

Received: September 24, 2012
Published online: January 17, 2013

Keywords: carbides · cellulose · ink-jet printing · iron · printed electronics

[1] L. Venema, *Nature* **2011**, *479*, 309 – 309.
[2] H. Sirringhaus, T. Kawase, R. H. Friend, T. Shimoda, M. Inbasekaran, W. Wu, E. P. Woo, *Science* **2000**, *290*, 2123 – 2126.
[3] a) W. Mueannoom, A. Srisongphan, K. M. G. Taylor, S. Hauschild, S. Gaisford, *Eur. J. Pharm. Biopharm.* **2012**, *80*, 149 – 155; b) S. Hauschild, U. Lipprandt, A. Rumplecker, U. Borchert, A. Rank, R. Schubert, S. Förster, *Small* **2005**, *1*, 1177 – 1180.
[4] M. Lejeune, T. Chartier, C. Dossou-Yovo, R. Noguera, *J. Eur. Ceram. Soc.* **2009**, *29*, 905 – 911.
[5] J. A. Hiller, J. D. Mendelsohn, M. F. Rubner, *Nat. Mater.* **2002**, *1*, 59 – 63.
[6] J. T. Delaney, Jr., A. R. Liberski, J. Perelaer, U. S. Schubert, *Macromol. Rapid Commun.* **2010**, *31*, 1970 – 1976.
[7] a) J. H. Cho, J. Lee, Y. Xia, B. Kim, Y. He, M. J. Renn, T. P. Lodge, C. D. Frisbie, *Nat. Mater.* **2008**, *7*, 900 – 906; b) H. Yan, Z. Chen, Y. Zheng, C. Newman, J. R. Quinn, F. Dotz, M. Kastler, A. Facchetti, *Nature* **2009**, *457*, 679 – 686; c) H. Minemawari, T. Yamada, H. Matsui, J. y. Tsutsumi, S. Haas, R. Chiba, R. Kumai, T. Hasegawa, *Nature* **2011**, *475*, 364 – 367; d) E. Tekin, P. J. Smith, U. S. Schubert, *Soft Matter* **2008**, *4*, 703 – 713.
[8] F. Torrisi, T. Hasan, W. Wu, Z. Sun, A. Lombardo, T. S. Kulmala, G.-W. Hsieh, S. Jung, F. Bonaccorso, P. J. Paul, D. Chu, A. C. Ferrari, *ACS Nano* **2012**, *6*, 2992 – 3006.
[9] O. P. Krivoruchko, V. I. Zaikovskii, *Kinet. Catal.* **1998**, *39*, 561 – 570.
[10] X. Feng, S. W. Chee, R. Sharma, K. Liu, X. Xie, Q. Li, S. Fan, K. Jiang, *Nano Res.* **2011**, *4*, 767 – 779.
[11] K. Jiang, C. Feng, K. Liu, S. Fan, *J. Nanosci. Nanotechnol.* **2007**, *7*, 1494 – 1504.
[12] J. Y. Yuan, C. Giordano, M. Antonietti, *Chem. Mater.* **2010**, *22*, 5003 – 5012.

